AJNR

Diagnostic Value of Sylvian Fissure Hyperechogenicity in Fetal SAH

M. Zhang, H. Wen, M. Liang, Y. Qin, Q. Zeng, D. Luo, X. Zhong and S. Li

Diagnostic Value of Sylvian Fissure Hyperechogenicity in Fetal SAH

M. Zhang, H. Wen, M. Liang, Y. Qin, Q. Zeng, D. Luo, X. Zhong, and S. Li

ABSTRACT

BACKGROUND AND PURPOSE: Fetal SAH is an intracranial malformation. The typical diagnostic features of fetal SAH in ultrasound have not been reported. This study aimed to evaluate the diagnostic value of Sylvian fissure hyperechogenicity by prenatal ultrasound in fetuses with SAH.

MATERIALS AND METHODS: The features on ultrasound and MR imaging of 10 fetuses with SAH were reviewed and summarized. The diagnostic value of the Sylvian fissure in fetal SAH by prenatal ultrasound was evaluated.

RESULTS: The typical and most obvious manifestations of SAH during the prenatal period were hyperechogenicity in the subarachnoid cavity, especially in the Sylvian fissure; all 10 cases (10/10) had such manifestations. Other manifestations included a hyperecho in other sulci (6/10), especially in the subfrontal sulcus, superior temporal sulcus, or parieto-occipital sulcus; a hyperecho in the cisterns (8/10), especially in the suprasellar cistern, posterior cranial fossa, cisterna ambiens, or quadrigeminal cistern; and a hyperecho around the anterior and posterior longitudinal fissures (2/10). Combined hemorrhage in the parenchymal layer or ventricles (9/10) was found. In addition, Doppler ultrasound showed that the peak flow velocity in the MCA increased in 6 cases (6/10).

CONCLUSIONS: The homogeneous hyperechogenicity of the Sylvian fissure is an important clue for detecting and diagnosing fetal SAH by prenatal ultrasound. A diagnostic approach has been proposed for fetal SAH, which has great significance in further prognosis.

ABBREVIATIONS: SF = Sylvian fissure; US = ultrasound

F etal SAH is considered a finding of blood flow into the subarachnoid space after the rupture of a blood vessel at the base or on the surface of the brain. It is one of the forms of nongerminal stromal hemorrhage, with an estimated incidence of less than 0.5–0.9 per 1000 pregnancies; however, its pathogenesis remains unclear.[1] It not only causes fetal stroke, fetal brain injury, and other diseases but is closely related to postpartum epilepsy, mental disorders, psychomotor retardation, cerebral palsy, and other neurologic disorders.[2] At present, few cases of fetal SAH have been reported at home and abroad.[3-11] In addition, the diagnosis of fetal SAH by prenatal ultrasound (US) has not been mentioned at all. Ten cases of fetal SAH were detected during a 3-year period at Shenzhen Maternity & Child Healthcare Hospital. Awareness of the diagnostic criteria, especially the characteristics of ultrasound of the Sylvian fissure (SF), disease progression, combined malformations, and further prognosis, is necessary for informed prenatal counseling and obstetric management. The related literature of fetal SAH for nearly 30 years was systematically discussed in this study.

MATERIALS AND METHODS
Research Design and Patients

We detected 10 gravidas with fetal SAH undergoing routine prenatal scanning between January 2018 and April 2021. Ethics approval for this study was by the regional ethical review board in Shenzhen: approval number: SFYLS [2020] 019 (decision 2020-06-11).
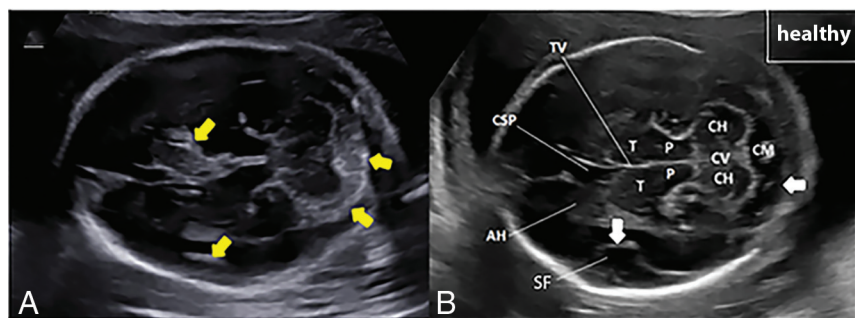
FIG 1. Transcerebellar plane of US in SAH and healthy fetuses. *A*, Echo in the subarachnoid space of fetal SAH was enhanced and widened. Hyperechoic filling could be seen in the SF; uneven strong echo masses could be seen in anterior parenchyma of the thalamus and around the ependyma; and hyperechoic filling could be seen in the posterior cranial fossa (*yellow arrows*). *B*, In healthy fetuses, the SF and posterior cranial fossa are homogeneous hypoechos (*white arrows*). TV indicates third ventricle; CSP, cavity of septum pellucidum; AH, anterior horn of lateral ventricle; T, thalamus; P, mesencephalon; CH, cerebellar hemisphere; CV, cerebellar vermis; CM, cisterna magna.
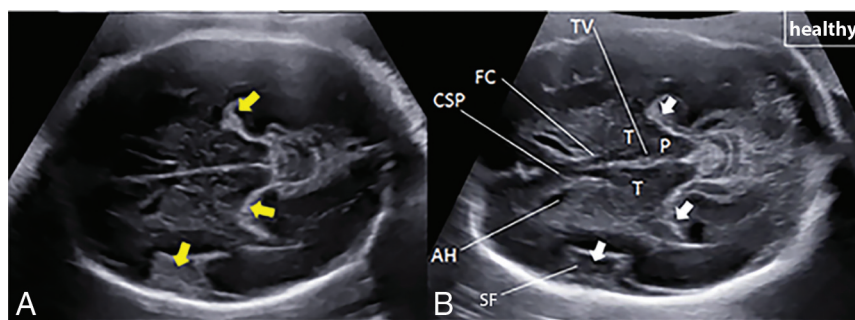

FIG 2. Transthalamic plane of US in SAH and healthy fetuses. *A*, The SF and temporal angle are filled with coarse hyperecho in the fetus with SAH (*yellow arrows*). *B*, In healthy fetuses, the SF is hypoechoic with narrow and sharp hyperechoic lines on both sides of the posterior midbrain (*white arrows*). TV indicates third ventricle; CSP, cavity of septum pellucidum; AH, anterior horn of lateral ventricle; T, thalamus, P, mesencephalon; FC, fornix column.

Materials Used

The scanning was performed by experienced radiologists using WS80A (Samsung Health) and S60 (SonoScape Health) equipped with transabdominal transducers (CA1-7A [Samsung Health]; CV1-8A [Samsung Health] and C1-6A [SonoScape Health] MHz).

Means of Confirming Diagnoses

Ultrasonic images of the fetal SAH were collected by 2 researchers, one with >20 years' experience in fetal sonography (Dr Li) and the other with only 2 years (Dr Zhang). All examinations were performed in real time, digitally stored, and documented using a commercially available system.

The routine cerebral survey included a detailed anatomic ultrasound survey of the fetal head. Fetal cerebrum views were routinely obtained in the transverse views of the thalamus plane, the lateral ventricle plane, and the cerebellum plane. If the fetal SF showed hyperechogenicity, additional views, including transverse, coronal, and sagittal sections of the fetal head from the parietal bone to the skull base, were needed to observe other cerebral sulci and cisterns dynamically, which mainly contained the superior

frontal sulcus, inferior frontal sulcus, supratemporal sulcus, inferior temporal sulcus, parieto-occipital sulcus in the sulci and the posterior cranial fossa, cisterna ambiens, and suprasellar cistern in the cisterns. If homogeneous hyperechoic or subarachnoid dilation was visualized, SAH was considered and MR imaging or genetic testing was recommended. All the screening procedures were performed on 2 sides of the brain to prevent a missed diagnosis. Furthermore, dynamic scanning was performed at the midsagittal view of the spine to obtain more findings in the subarachnoid space. At the same time, color Doppler was used to measure the peak flow velocity of the MCA to search for the possible causes of SAH.

All suspected patients were recommended for MR imaging in 2–5 days. Fetuses with an abnormal subarachnoid echo on the prenatal examination were recommended for follow-up perinatal outcome and prognosis.

Statistical Analysis

Interobserver agreement with regard to the observation of the SAH sites was determined as κ coefficients and P values, according to the κ methods. Statistical analyses were performed using SPSS 20.0 for Windows (IBM). Basic descriptive statistics were performed when appropriate. The diagnostic utility of SF hyperechogenicity for the diagnosis of fetal SAH was determined by calculating the detection rate for consensus reader data.

RESULTS

Incidence

Fetal SAH was detected in 10 cases of 425,258 deliveries (0.23/10,000 deliveries) at the authors' institution between January 2018 and April 2021. The incidence was probably biased because of the diagnosis of fetal SAH that required specific expertise, and the actual incidence of SAH might be higher. The mean maternal age was 29.3 (SD, 4.3) years (range, 26–38 years). The mean gestational age at diagnosis was 28.6 (SD, 4.6) weeks (range, 23–36 weeks).

Results of Prenatal Examinations

The typical and most obvious manifestation of SAH in prenatal diagnoses was hyperechogenicity in the subarachnoid cavity, especially in the SF; all 10 cases (10/10) had such manifestations (Figs 1–3). Other manifestations included thick hyperechogenicity in the other sulci (6/10), especially in the subfrontal sulcus, superior temporal sulcus, or parieto-occipital sulcus (Figs 3 and
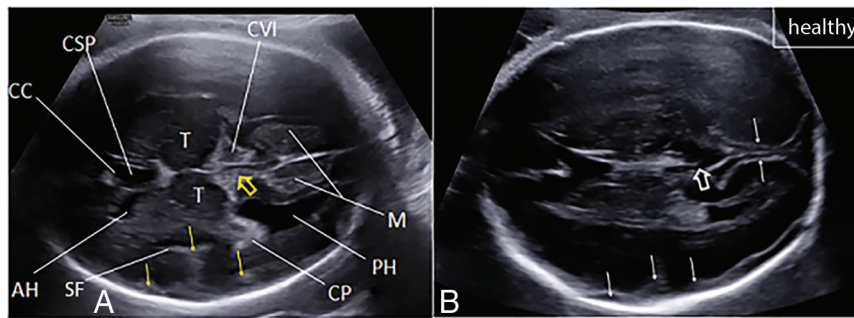
FIG 3. Transventricular plane of US in SAH and healthy fetuses. *A*, Hyperecho inside the cerebral sulci, such as the subfrontal sulcus, the SF, and the superior temporal sulcus, can be seen in the fetus with SAH, and the boundary is blurred (*small yellow arrow*). There is an enhanced echo in the cavum veli interpositi (*yellow hollow arrow*) and symmetric isoechoic or slightly hyperechoic hemorrhagic foci (M) around the parafalx anterior to the sinus confluence. Compression of the cerebral parenchyma is seen. *B*, In healthy fetuses, a clear hypoecho in the subarachnoid spaces in the SF, the superior temporal sulcus and subfrontal sulcus (*small white arrow*), and cavum veli interpositi (*white hollow arrow*); a normal cerebral falx; and no compression are observed in brain parenchyma. CC indicates corpus callosum; CSP, cavity of septum pellucidum; CVI, cavum veli interpositi; PH, posterior horn of lateral ventricle; CP, choroid plexus; AH, anterior horn of lateral ventricle; T, thalamus; M, subdural hemorrhage was suspected.
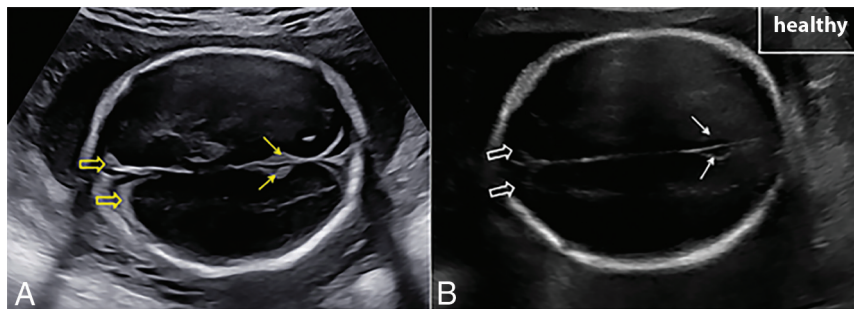

FIG 4. The transcalvarial plane of US in SAH and healthy fetuses. *A*, Abnormal hyperecho in the parieto-occipital sulcus of the fetus with SAH, with blurred boundaries (*yellow arrows*). The enhanced echo and blurred boundary between the superior sagittal sinus and the parenchyma are thickened (*yellow hollow arrows*). *B*, In healthy fetuses, only the midline of the brain is clear in the parieto-occipital sulcus, and both sides of the sulcus are filled with clear anechoic CSF (*white arrows*). The superior sagittal sinus is clearly demarcated from the pericerebral parenchyma, showing a clear isoechoic line (*white hollow arrows*).
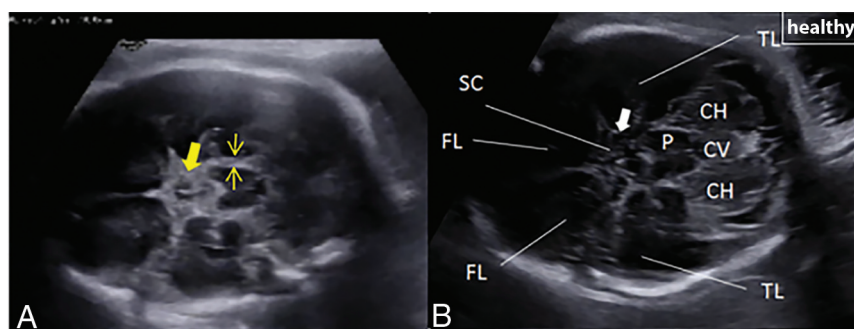

FIG 5. Transbasicranial plane of US in SAH and healthy fetuses. *A*, The suprasellar cistern and ambient cistern of the fetus with SAH show hyperecho (*yellow thick arrow*). Compared with the healthy fetus, the cistern was significantly widened and enhanced (*yellow thin arrows*). *B*, The suprasellar cistern and ambient cistern of a healthy fetus show hypoechoic or echoless (*white arrow*). SC indicates suprasellar cistern; TL, temporal lobe; FL, frontal lobe; CV, cerebellar vermis; CH, cerebellar hemisphere; P, mesencephalon.

4); hyperecho in the cisterns (8/10), especially in the suprasellar cistern, posterior cranial fossa, cisterna ambiens, or quadrigeminal cistern (Figs 1 and 5); hyperecho around the anterior and posterior longitudinal fissures (2/10) (Figs 3 and 4); combined hemorrhage in the parenchymal layer or ventricles (9/10) (Fig 1); and the hyperechoic dilated subarachnoid space in the middle view of the spine (1/10) (Fig 6). In addition, Doppler US showed that the peak flow velocity in the MCA increased obviously in 6 cases (6/10). Using this method and diagnostic features, we found that the κ number for the assessment was high, up to 0.82 ($P < .05$). An abnormal SF was visualized in all cases by the 2 researchers with different experience (Table).

Fetuses (5/10) underwent MR imaging 2–5 days after US, and all were diagnosed with SAH. Fetuses (6/10) underwent fetal chromosomal microarray analysis, which indicated negative results. The peak flow velocity of the MCA increased in fetuses (6/10). It was >1.55 and 1.29 multiples of the median (MOM) in 4 and 2 cases, respectively; mild and severe anemia were indicated, respectively. Neither of the parents had a history of blood diseases. In cases 1 and 5, the umbilical cord was wrapped 3 times around the neck. Twin-to-twin transfusion syndrome (phase IV) was found in case 7 of twins.

Perinatal Outcome

Six pregnancies with fetal SAH were induced after prenatal counseling and confirmed by postmortem examination (Fig 7). Two cases were intrauterine death and the rest were in pregnancy. The postmortem and imaging results showed that the novel diagnostic method with SF hyperechogenicity as the main clue had reached a detection rate of 100% (10/10).

DISCUSSION

In the normal SF and other sulci, cisterns are filled with anechoic CSF. When SAH occurs, the blood rarely forms a localized or encapsulated hematoma but flows along the CSF to low-lying areas, including some brain sulci and cisterns, owing to the
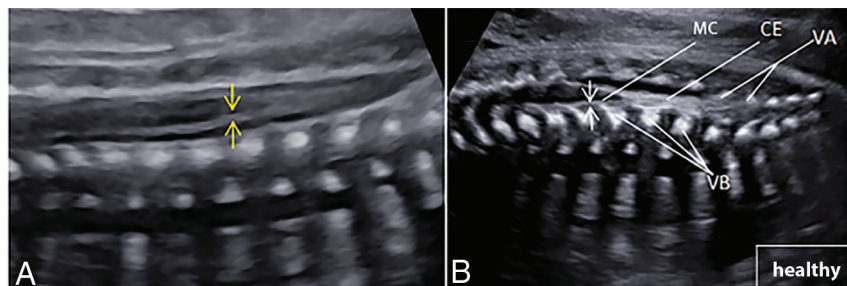
FIG 6. The midsagittal view of the spine on a sonogram in SAH and healthy fetuses. *A*, There are uniform thickening and a strong echo in the subarachnoid space between the pia mater spinalis and the arachnoid membranes of fetal SAH (*yellow arrows*). *B*, The normal fetal pia mater and arachnoid membrane are relatively close, forming a narrow space (*white arrows*). MC indicates medullary cone; CE, cauda equina; VA, vertebral arch; VB, vertebral body.

Comparison of intraobserver assessment in 10 cases

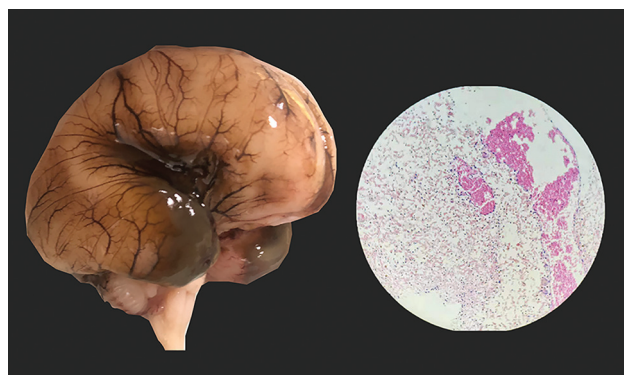| SAH Sites	Observer A	Observer B	κ (A and B)
Sylvian fissure	10	10	
Parieto-occipital sulcus	6	6	
Superior frontal sulcus	3	2	
Superior temporal sulcus	3	2	
Quadrigeminal cistern	7	6	
Posterior cranial fossa	8	7	
Suprasellar cistern	8	6	
Cisterna ambiens	8	7	
Longitudinal fissures	2	1	
Spinal subarachnoid space	1	0	
Total count	56	47	0.819 (*P* < .05)

FIG 7. Postmortem examination results and pathology. Hematoceles are seen in the SF and subarachnoid space of the temporal horn. The left image shows the cerebral postmortem examination of the fetus with SAH; the right image shows large amounts of remote bleeding in the SF in pathologic findings.

influence of gravity and arterial pulsation. The factors predisposing to fetal SAH include a variety of conditions, mostly maternal trauma and fetal coagulation disorders.[1,12] In many cases, however, the cause is not identified. Most fetal SAHs were usually considered spontaneous bleeding without a potential cause. However, previous studies[13-14] reported that fetal SAH might be related to *COL4A1* and *GATA1* gene mutations, but some reports[15-16] had normal outcomes.

Ultrasonography is the preferred imaging method for the prenatal diagnosis of SAH. Previous findings on the capacity of ultrasound to diagnose fetal SAH have been inconsistent. In this study, the 12 cases of fetal SAH for the past 30 years were reviewed in 9 published studies (Online Supplemental Data).[3-11] However, only 2 cases were diagnosed by US due to the lack of the description of ultrasonographic characteristics and diagnostic approaches in previously published studies.[6,10] Fetal SAH was still prone to missed diagnoses and misdiagnosis.

The SF is the earliest and largest sulcus shown on prenatal US, which can be observed at 18–20 weeks' gestation. The parieto-occipital sulcus and cisterns also appear earlier, but they need to be visualized at the specific section and angle. The other sulci of the subarachnoid space can be displayed much later.[17,18] For example, generally, the superior temporal sulcus and inferior frontal sulcus appear at 31 weeks' gestation.[17,19]

The SF is an excellent structure for diagnosing SAH. In our case, the earliest gestational age in SAH diagnosis was 23 weeks. However, theoretically, it was believed that fetal SAH could be diagnosed as early as 18 weeks according to the visualization of the SF in fetuses. The characteristics of the SF were the direct evidence indicating that SAH had occurred. Previous studies focused on the morphology of the sulci, especially the SF, to assess cortical development rather than the internal sonography of the sulci.[19,20] In this study, the hyperechoic US features within the SF were detected as the most intuitive, which served as an essential clue to the diagnosis of fetal SAH. Furthermore, a 100% (10/10) rate of appearance of a hyperechoic SF was detected by the 2 observers in all cases. Other sulci (6/10) and cisterns (8/10) were also seen with the hyperecho in them. The analysis of detection by the 2 observers is summarized in the Table. The κ number for the 2 observers with different seniority was 0.82 (*P* < .05), which showed good repeatability and agreement on the diagnostic characteristics and methods.

In the 8 cases before 31 weeks' gestation, only 1 case showed SAH in the superior temporal sulcus and inferior frontal sulcus because most sulci could rarely be detected before 31 weeks' gestation.[19] Therefore, a focus on the observation of the SF, parieto-occipital sulcus, and cisterns before 31 weeks was recommended. The diagnosis at the third trimester might be disturbed by SF operculization with an unclear intrafissural hyperecho. Dynamic scanning could make a multiangle observation of the SF, other sulci, and cisterns. Therefore, in SF operculization or a doubtful situation, other cerebral planes should be added dynamically besides the 3 cerebral screening axial planes when hyperechogenicity is found within the SF. The echo of the sulci and cisterns should also be observed, such as the superior temporal sulcus, parieto-occipital sulcus, posterior cranial fossa, and cisterna ambiens. Furthermore, the anterior and posterior longitudinal fissures and the spinal

subarachnoid space should also be examined for further evidence of fetal SAH. Two cases of SAH in the longitudinal fissure and 1 in the spinal subarachnoid space were detected; all these cases were associated with intraparenchymal hemorrhage, intraventricular hemorrhage, or SAH. It was recommended that the anterior and posterior longitudinal fissure and the spinal subarachnoid space of fetuses, combined with intraparenchymal hemorrhage, intraventricular hemorrhage should be visualized, not just the common sulci and cisterns in the brain. At the same time, this study and previous studies suggested that SAH was usually associated with an increased peak flow rate of the MCA, implicating different degrees of anemia in fetuses (6/10).[21] Spectral Doppler in the MCA might help determine the cause.

However, once the SAH clot has formed, it might cause CSF obstruction and lead to chronic hydrocephalus or cerebral edema, affecting the blood supply and causing cerebral function damage, which should be well-noted in fetal SAH.

On the basis of the straightforward and intuitive diagnostic features and method, the detection rate of fetal SAH was up to 100% (10/10); the SF hyperecho was the best indicator of SAH diagnosis in prenatal US.

MR imaging should be recommended once US suggests the presence of fetal SAH. It is primarily found in the subacute phase on MR imaging, showing a high signal on T1WI and a low signal on T2WI. However, the partial volume effect and dilution of CSF with a higher partial pressure of oxygen make the detection of SAH difficult on MR imaging using conventional sequences. Uncontrolled fetal movement makes MR imaging diagnosis more challenging.

Considering the aforementioned reasons, in the present study, the US diagnosis was confirmed by MR imaging (5/10), indicating that the signal changes were seen in tiny sulci but no definite signs in the SF, leading to higher diagnostic difficulty and misdiagnosis rates compared with US for fetal SAH.

The differential diagnosis of hyperechoic or heterogeneous hyperechoic intracranial lesions includes tumor, calcification, hemangioma, and so forth. Tumors compress the adjacent brain tissue, and the mass shows little change or only gradual enlargement with time. Color Doppler can be used to explore rich blood flow.[12,22] Calcification is mostly present as a dot or block hyperecho but with no obvious dynamic change.[23]

Perinatal SAH can cause seizures, apneas, and nervous system abnormalities, such as drowsiness and bregma.[24-26] Studies[3,5] showed certain neurologic symptoms in 2 cases (2/12) with a follow-up of 4–20 months. However, most of our cases were induced (8/10); only 2 cases with the gradual absorption of bleeding had a follow-up of 1–2 months after birth with no symptoms. Some scholars[1,2] believed that fetal SAH was rare and occurred at a relatively early gestational age, leading to a higher risk of severe sequelae or perinatal death. Previous studies and our study also demonstrated high induction (11/22) and death rates (7/22). In the neonatal period, consensus[24-26] was reached that neonates with isolated SAH had a good prognosis generally, but the site and degree of bleeding were considered, too.

At present, the reported results may vary significantly due to the lack of a prenatal diagnosis and case reports of fetal SAH and insufficient follow-up data. Also, the prognosis may need to be inferred from neonatal SAH according to the etiology and medical history for further prenatal consultation and management.

CONCLUSIONS

Fetal SAH can be diagnosed by prenatal US due to its unique sonographic characteristics. SF hyperechogenicity is recommended as a significant clue. Prenatal US is used to observe the SF and other sulci and cisterns from conventional transverse planes or in coronal and sagittal sections dynamically. If combined cerebral hemorrhage occurs, the spinal subarachnoid space and the longitudinal fissure are continuously viewed. This kind of method has great significance in assessing bleeding degrees and further prognosis. At present, case reports of fetal SAH are lacking; hence, future studies should aim to collect more cases and test the proposed novel diagnostic method for further stages.

REFERENCES

1. Ghi T, Simonazzi G, Perolo A, et al. **Outcome of antenatally diagnosed intracranial hemorrhage:case series and review of the literature.** *Ultrasound Obstet Gynecol* 2003;22:121–30 CrossRef Medline

2. Sanapo L, Whitehead MT, Bulas DI, et al. **Fetal intracranial hemorrhage: role of fetal MRI.** *Prenat Diagn* 2017;37:827–36 CrossRef Medline

3. Bowdler N, Faix RG, Elkins T. **Fetal skull fracture and brain injury after a maternal automobile accident: a case report.** *J Reprod Med* 1987;32:375–78 Medline

4. Govaert P, Bridger J, Wigglesworth J. **Nature of the brain lesion in fetal allo-immune thrombocytopenia.** *Dev Med Child Neurol* 1995;37:485–95 CrossRef Medline

5. Hagmann CF, Schmitt-Mechelke T, Caduff JH, et al. **Fetal intracranial injuries in a preterm infant after maternal motor vehicle accident: a case report.** *Pediatr Crit Care Med* 2004;5:396–98 CrossRef Medline

6. Kidron D, Tepper R, Beyth Y, et al. **Superficial hemosiderosis in a second trimester fetus: pathological and clinical manifestations.** *Hum Pathol* 1995;26:1038–40 CrossRef Medline

7. Nishida N, Ina S, Hata Y, et al. **Fetal closed head injuries following maternal motor vehicle accident: a clinicopathologic case report.** *Medicine (Baltimore)* 2018;97:e13133 CrossRef Medline

8. Stafford PA, Biddinger PW, Zumwalt RE. **Lethal intrauterine fetal trauma.** *Am J Obstet Gynecol* 1988;159:485–89 CrossRef Medline

9. Tattoli L, Di Vella G, Solarino B. **A case of intrauterine lethal fetal injury after attempted suicide of the mother.** *Forensic Sci Int* 2017;280:e1–e5 CrossRef Medline

10. Tongsong T, Puntachai P, Tongprasert F, et al. **Sonographic findings in an isolated widened fetal subarachnoid space.** *J Ultrasound Med* 2015;34:917–24 CrossRef Medline

11. Zanders EH, Buist FC, van Vugt JM. **Prenatal diagnosis of fetal intracranial hemorrhage at 25 weeks of gestation.** *Fetal Diagn Ther* 2003;18:324–27 CrossRef Medline

12. Putbrese B, Kennedy A. **Findings and differential diagnosis of fetal intracranial haemorrhage and fetal ischaemic brain injury: what is the role of fetal MRI?** *Br J Radiol* 2017;90:2016025 CrossRef Medline

13. Bouchghoul H, Quelin C, Loget P, et al. **Fetal cerebral hemorrhage due to X-linked GATA1 gene mutation.** *Prenat Diagn* 2018;38:772–78 CrossRef Medline

14. Kutuk MS, Balta B, Kodera H, et al. **Is there relation between COL4A1/A2 mutations and antenatally detected fetal intraventricular hemorrhage?** *Childs Nerv Syst* 2014;30:419–24 CrossRef Medline

15. Elchalal U, Yagel S, Gomori JM, et al. **Fetal intracranial hemorrhage (fetal stroke): does grade matter?** *Ultrasound Obstet Gynecol* 2005;26:233–43 CrossRef Medline

16. Martino F, Malova M, Cesaretti C, et al. **Prenatal MR imaging features of isolated cerebellar haemorrhagic lesions.** *Eur Radiol* 2016;26:2685–96 CrossRef Medline

17. Girard N, Raybaud C, Gambarelli D, et al. **Fetal brain MR imaging.** *Magn Reson Imaging Clin N Am* 2001;9:19–56, vii CrossRef Medline

18. Levine D, Barnes PD. **Cortical maturation in normal and abnormal fetuses as assessed with prenatal MR imaging.** *Radiology* 1999;210:751–58 CrossRef Medline

19. Chen X, Li SL, Luo GY, et al. **Ultrasonographic characteristics of cortical sulcus development in the human fetus between 18 and 41 weeks of gestation.** *Chin Med J (Engl)* 2017;130:920–28 CrossRef Medline

20. Guibaud L, Selleret L, Larroche JC, et al. **Abnormal Sylvian fissure on prenatal cerebral imaging: significance and correlation with neuropathological and postnatal data.** *Ultrasound Obstet Gynecol* 2008;32:50–60 CrossRef Medline

21. Mari G, Deter RL, Carpenter RL, et al. **Noninvasive diagnosis by Doppler ultrasonography of fetal anemia due to maternal red-cell alloimmunization: collaborative group for Doppler assessment of the blood velocity in anemic fetuses.** *N Engl J Med* 2000;342:9–14 CrossRef Medline

22. Bin C, Jun Z. **MRI characteristics fetal intracranial hemorrhage in 120 cases.** *Chinese Journal of Magnet Resonance Imaging* 2019;10:491–96

23. Fukuyama Y, Osawa M, Suzuki H. **Congenital progressive muscular dystrophy of the Fukuyama type: clinical, genetic and pathological considerations.** *Brain Dev* 1981;3:1–29 CrossRef Medline

24. Gupta SN, Kechli AM, Kanamalla US. **Intracranial hemorrhage in term newborns: management and outcomes.** *Pediatr Neurol* 2009;40:1–12 CrossRef Medline

25. Tan AP, Svrckova P, Cowan F, et al. **Intracranial hemorrhage in neonates: a review of etiologies, patterns and predicted clinical outcomes.** *Eur J Paediatr Neurol* 2018;22:690–717 CrossRef Medline

26. Shah NA, Wusthoff CJ. **Intracranial hemorrhage in the neonate.** *Neonatal Netw* 2016;35:67–71 CrossRef Medline